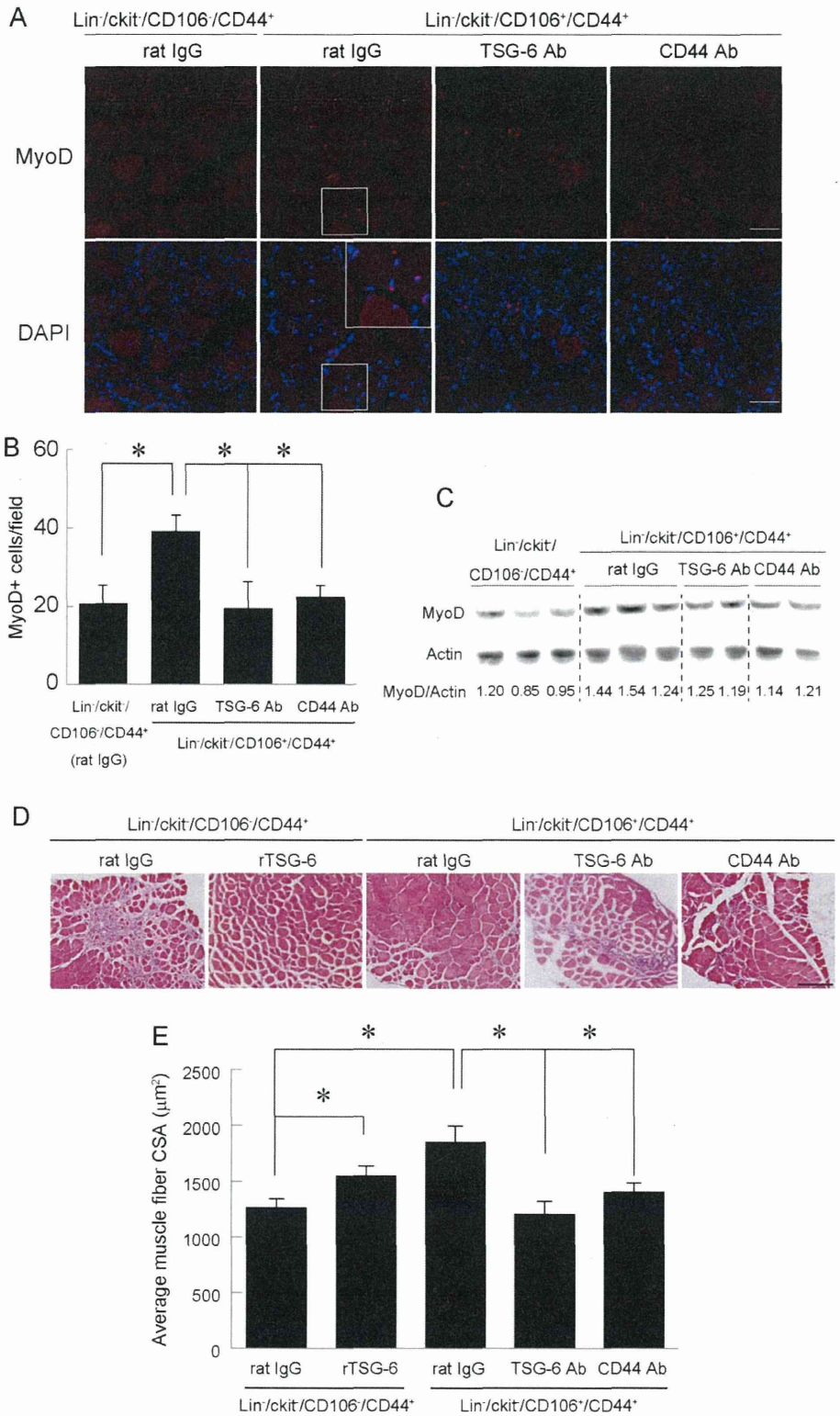

Figure 6. Effect of specific bone marrow-mesenchymal stromal cell populations on skeletal muscle regeneration. **(A):** Immunofluorescent staining for MyoD (red) on tibialis anterior (TA) muscle of Mdx-ckit$^+$ BMT mice 7 days post-treatment of Lin$^-$/ckit$^-$/CD106$^-$/CD44$^+$ or Lin$^-$/ckit$^-$/CD106$^+$/CD44$^+$ bone marrow cells (BMCs) in combination with either a CD44 antibody (KM81) or a TSG-6 antibody. Nuclei were stained with DAPI (blue). Scale bars = 50 μm. **(B):** MyoD$^+$ cells were quantified. The values are the mean ± SEM (n = 3–4/group); *, $p < .05$. **(C):** Western blot analyses of MyoD and Pan-actin (loading control) of TA muscles of Mdx-ckit$^+$ BMT mice at 7 days post-treatment of Lin$^-$/ckit$^-$/CD106$^-$/CD44$^+$ or Lin$^-$/ckit$^-$/CD106$^+$/CD44$^+$ BMCs in combination with either a CD44 antibody (KM81) or a TSG-6 antibody. Quantified band densities of MyoD normalized to actin are also shown. **(D):** H&E staining on TA muscle of Mdx-ckit$^+$ BMT mice 7 days post-treatment of Lin$^-$/ckit$^-$/CD106$^-$/CD44$^+$ or Lin$^-$/ckit$^-$/CD106$^+$/CD44$^+$ BMCs in combination with either recombinant TSG-6 or CD44 antibody (KM81) or TSG-6 antibody. Scale bar = 200 μm. **(E):** The average CSA of muscle fibers with central nuclei was quantified. The values are the mean ± SEM (n = 4–8/group); *, $p < .05$. Abbreviation: CSA, cross-sectional area.

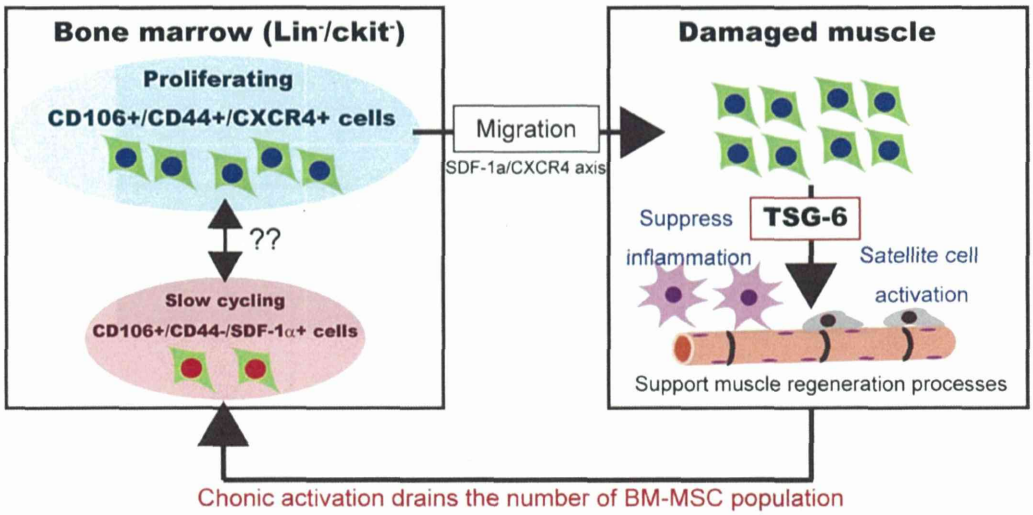

Figure 7. *Schematic summary of the present findings. The* Lin$^-$/ckit$^-$/CD106$^+$/CD44$^+$ *BMC population abundantly migrates into damaged muscles to suppress inflammation and activate the muscle regeneration processes in Duchenne muscular dystrophy, in part via the TSG-6-mediated pathway. Chronic injury/regeneration cycles drain the numbers of both* Lin$^-$/ckit$^-$/CD106$^+$/CD44$^+$ *and* Lin$^-$/ckit$^-$/CD106$^+$/CD44$^-$ *populations in BM. Abbreviation: BM-MSCs, bone marrow-mesenchymal stromal cells.*

Hagiwara et al. proposed that BMT did not significantly improve the muscle function of mdx mice [43] compared with non-BMT mdx mice, which is consistent with this study. For BMT, the recipient mice receive high-dose irradiation that ablates not only bone marrow cells but also other cells to worsen the regeneration ability. Therefore, in our study, we first conducted the 10-week-old mdx or WT mouse BMC transplantation into 3–4-week-old mdx mice (Mdx-wt vs. Mdx-mdx) to compare these two BMT models on mdx mouse pathology. Although muscle differentiation from BMCs was almost undetectable, we observed muscle function and pathological differences between these mice. From that point, we hypothesized and investigated whether the differences in the WT and mdx BM-MSC populations and the alteration of BM-MSC populations could be related to muscle pathological conditions in mdx mice.

Several possibilities could account for the reduction of BM-MSC populations in 10-week-old mdx mice. We previously reported that transient reduction of the CD45$^-$/CD44$^+$/CXCR4$^+$ cells in BM with appearance of this population in peripheral blood during ectopic bone formation [8]. In addition, during the inflammation phase in multiple sclerosis mice, interferon-gamma secreted from activated T cells decreased the number of CFU-Fs and CD45$^-$ cells in BM [44]. These data suggest that induction of direct or indirect stimuli in pathological conditions can mobilize MSC populations from BM to contribute to tissue regeneration at a distant location. In mdx mice, these stimuli from degenerated muscles are expected to chronically continue because the muscle pathological symptoms have progressed. Thus, the continuous requirement to contribute to muscle regeneration from BM might be responsible for the reduction in the BM-MSC population in mdx mice (Fig. 7). Previously, we reported that HMGB1 is abundantly released from necrotic epithelial cells of the mouse skin graft model and mobilizes PDGFR$^+$ cells from BM into the circulation [9]. In DMD mice, however, we did not observe HMGB1 elevation in the serum (data not shown), indicating another unknown mechanism underlying the mobilization of BM-MSCs from BM into circulation and damaged muscles.

Surface marker analyses have suggested the existence of multiple subpopulations in BM-MSCs [15, 16], and the roles of each population in vivo have remained unclear. Here, we demonstrated that BM-MSCs can be subdivided into Lin$^-$/ckit$^-$/CD106$^+$/CD44$^+$ and Lin$^-$/ckit$^-$/CD106$^+$/CD44$^-$ cells. Our whole-transcriptome analysis demonstrated that the Lin$^-$/ckit$^-$/CD106$^+$/CD44$^-$ cells preferentially expressed SDF-1α in BM. SDF-1α-expressing stromal cells in BM contribute to niche formation for HSCs [10, 13, 14, 45]. In addition, there are some similarities in the expression profiles of other genes between Lin$^-$/ckit$^-$/CD106$^+$/CD44$^-$ BMCs and CXCL12 (SDF-1α)-abundant reticular cells or niche-maintaining cells in BM [10–12, 14, 46]. From this context, we estimate that Lin$^-$/ckit$^-$/CD106$^+$/CD44$^-$ cells in BM may be involved in this niche formation mechanism for HSCs. Further precise investigations are necessary to elucidate the roles and functions of this mesenchymal cell population in BM.

Similar to HSC, heterogeneous MSC populations are also hierarchically organized at the apex, from stem-like cells with self-renewing capacity to more differentiated cells with limited lineage potentials [15, 16]. The stem cell populations in various tissues are generally thought to be in a slow cycling or quiescence state under physiological conditions [47–49]. In this study, the Lin$^-$/ckit$^-$/CD106$^+$/CD44$^+$ population was proliferative and dominantly accumulated in damaged muscles. Conversely, the Lin$^-$/ckit$^-$/CD106$^+$/CD44$^-$ population in BM was shown to be a slow-cycling population. Thus, it appears that the Lin$^-$/ckit$^-$/CD106$^+$/CD44$^+$ population includes effecter cells that egress into the circulation in response to injury and serve to support regeneration through their anti-inflammatory activity and resident stem-cell activation, whereas the Lin$^-$/ckit$^-$/CD106$^+$/CD44$^-$ population in BM includes a stem-like cell population. However, it is still unclear whether a hierarchical relationship between Lin$^-$/ckit$^-$/

$CD106^+/CD44^-$ and $Lin^-/ckit^-/CD106^+/CD44^+$ BMCs (Fig. 7) exists, and further studies are warranted to clarify the in vivo relationship of these two populations.

In a recent study, CD106 marked an MSC subpopulation with unique and powerful immunomodulatory activities in vitro [6]. However, no report is available for the in vivo function of $CD106^+$ MSCs. This study showed that recruited $Lin^-/ckit^-/CD106^+/CD44^+$ BMCs highly expressed TSG-6 in damaged muscle. TSG-6 is a strong anti-inflammatory protein that is secreted from MSCs in culture [3, 42, 50–52]. We also showed that the TSG-6- or TSG-6/CD44-mediated pathway activates myoblast and satellite cells in vitro and in vivo. In addition, we observed the acceleration of muscle regeneration as well as the suppression of inflammation following the treatment of freshly isolated $Lin^-/ckit^-/CD106^+/CD44^+$ BMCs, in part through the TSG-6-mediated pathway. However, we cannot yet determine the benefits of $Lin^-/ckit^-/CD106^+/CD44^-$ BMCs for damaged muscles. Although the accumulation of $Lin^-/ckit^-/CD106^+/CD44^-$ BMCs is low in mdx muscles, these cells may have a high impact on the muscle regeneration process. Therefore, in future studies, it would be of interest to investigate whether this small BM-MSCs fraction ($Lin^-/ckit^-/CD106^+/CD44^-$) has the same effect on muscle regeneration as observed in $Lin^-/ckit^-/CD106^+/CD44^+$ BMCs or whether they exhibit different activities, such as muscle differentiation.

In this study, we did not consider the potential effect of $Lin^-/ckit^-/CD106^+/CD44^+$ BMCs or TSG-6 on muscle resident fibro/adipocyte progenitors (FAPs). Recent studies have indicated that sufficient FAPs activities are important for muscle regeneration [53–55]. It is also known that BM-MSCs and FAPs have similar surface markers [54, 55] and express CD44 [56, 57], thus suggesting that TSG-6 secreted from $Lin^-/ckit^-/CD106^+/CD44^+$ BMCs also has effects on FAP proliferation and activities to facilitate muscle regeneration. The interaction of BM-MSCs with FAPs during muscle regeneration needs to be investigated precisely in the future. Together, these findings illustrate the putative scheme for the roles of the BM-derived $Lin^-/ckit^-/CD106^+/CD44^+$ BMCs, which dominantly migrate in damage muscles and release TSG-6, with other trophic factors, to suppress inflammation/fibrosis and promote muscle regeneration processes in vivo. With future studies, the local/systemic administration of TSG-6 may become a new candidate strategy for improving DMD pathology.

Conclusions

In conclusion, it is clear that the normalization of dystrophin gene expression is necessary for the ultimate cure of DMD. Nevertheless, we consider that the series of results shown here have a significant impact on the muscle repair mechanisms by the endogenous BM-MSC population. This study also provides a novel concept that the normalization of MSC populations in BM may prevent the secondary exacerbation of inflammatory/fibrotic damages and improve clinical manifestations. A chronic exhaustion of MSC populations in BM appears to occur in other intractable hereditary or nonhereditary diseases besides DMD if persistent injury and inflammation continuously activate $Lin^-/ckit^-/CD106^+/CD44^+$ cells in BM. Further precise analyses of heterogeneous BM-MSC populations to understand their roles and mechanisms in various in vivo pathological settings may provide novel therapeutic strategies by targeting intrinsic homeostatic maintenance mechanisms driven by BM-MSCs in vivo.

Acknowledgments

R.F. was funded by a Research Fellowship (#243873) from the Japan Society for the Promotion of Science (JSPS), Japan. This study was also supported by a Grant-in-Aid for Scientific Research from the Ministry of Education, Culture, Sports, Science, and Technology of Japan and a Health and Labour Sciences Research Grant (Research of Intractable Diseases) from the Ministry of Health, Labour, and Welfare of Japan.

Author Contributions

R.F.: conception and design, performed experiments, collection and/or assembly of data, data analysis and interpretation, financial support, and manuscript writing; K.T.: conception and design, manuscript writing, financial support, and final approval of manuscript; E.A.: collection and/or assembly of data and data analysis and interpretation; K.N. and S.I.: data analysis and interpretation; Y. Kikuchi: administrative support and provision of study material; Y. Kaneda: conception and design, financial support, and final approval of manuscript.

Disclosure of Potential Conflicts of Interest

The authors indicate no potential conflicts of interest.

References

1 Pittenger MF, Mackay AM, Beck SC et al. Multilineage potential of adult human mesenchymal stem cells. Science 1999;284:143–147.

2 Prockop DJ. Marrow stromal cells as stem cells for nonhematopoietic tissues. Science 1997;276:71–74.

3 Lee RH, Pulin AA, Seo MJ et al. Intravenous hMSCs improve myocardial infarction in mice because cells embolized in lung are activated to secrete the anti-inflammatory protein TSG-6. Cell Stem Cell 2009;5:54–63.

4 Gupta N, Su X, Popov B et al. Intrapulmonary delivery of bone marrow-derived mesenchymal stem cells improves survival and attenuates endotoxin-induced acute lung injury in mice. J Immunol 2007;179:1855–1863.

5 Wu Y, Chen L, Scott PG et al. Mesenchymal stem cells enhance wound healing through differentiation and angiogenesis. StemCells 2007;25:2648–2659.

6 Yang ZX, Han ZB, Ji YR et al. CD106 identifies a subpopulation of mesenchymal stem cells with unique immunomodulatory properties. PLoS One 2013;8:e59354.

7 Otsuru S, Tamai K, Yamazaki T et al. Bone marrow-derived osteoblast progenitor cells in circulating blood contribute to ectopic bone formation in mice. Biochem Biophys Res Commun 2007;354:453–458.

8 Otsuru S, Tamai K, Yamazaki T et al. Circulating bone marrow-derived osteoblast progenitor cells are recruited to the bone-forming site by the CXCR4/stromal cell-derived factor-1 pathway. StemCells 2008;26:223–234.

9 Tamai K, Yamazaki T, Chino T et al. PDGFRalpha-positive cells in bone marrow are mobilized by high mobility group box 1 (HMGB1) to regenerate injured epithelia. Proc Natl Acad Sci USA 2011;108:6609–6614.

10 Sugiyama T, Kohara H, Noda M et al. Maintenance of the hematopoietic stem cell pool by CXCL12-CXCR4 chemokine signaling in bone marrow stromal cell niches. Immunity 2006;25:977–988.

11 Ding L, Morrison SJ. Haematopoietic stem cells and early lymphoid progenitors occupy distinct bone marrow niches. Nature 2013;495:231–235.
12 Ding L, Saunders TL, Enikolopov G et al. Endothelial and perivascular cells maintain haematopoietic stem cells. Nature 2012;481: 457–462.
13 Greenbaum A, Hsu YM, Day RB et al. CXCL12 in early mesenchymal progenitors is required for haematopoietic stem-cell maintenance. Nature 2013;495:227–230.
14 Morrison SJ, Scadden DT. The bone marrow niche for haematopoietic stem cells. Nature 2014;505:327–334.
15 Anjos-Afonso F, Bonnet D. Nonhematopoietic/endothelial SSEA-1+ cells define the most primitive progenitors in the adult murine bone marrow mesenchymal compartment. Blood 2007;109:1298–1306.
16 Sarugaser R, Hanoun L, Keating A et al. Human mesenchymal stem cells self-renew and differentiate according to a deterministic hierarchy. PLoS One 2009;4:e6498.
17 Qian H, Badaloni A, Chiara F et al. Molecular characterization of prospectively isolated multipotent mesenchymal progenitors provides new insight into the cellular identity of mesenchymal stem cells in mouse bone marrow. Mol Cell Biol 2013;33:661–677.
18 Qian H, Le Blanc K, Sigvardsson M. Primary mesenchymal stem and progenitor cells from bone marrow lack expression of CD44 protein. J Biol Chem 2012;287:25795–25807.
19 Sicinski P, Geng Y, Ryder-Cook AS et al. The molecular basis of muscular dystrophy in the mdx mouse: A point mutation. Science 1989;244:1578–1580.
20 Miyagoe-Suzuki Y, Takeda S. Gene therapy for muscle disease. Exp Cell Res 2010; 316:3087–3092.
21 Blake DJ, Weir A, Newey SE et al. Function and genetics of dystrophin and dystrophin-related proteins in muscle. Physiol Rev 2002;82:291–329.
22 Partridge TA, Morgan JE, Coulton GR et al. Conversion of mdx myofibres from dystrophin-negative to -positive by injection of normal myoblasts. Nature 1989;337:176–179.
23 Skuk D, Paradis M, Goulet M et al. Intramuscular transplantation of human postnatal myoblasts generates functional donor-derived satellite cells. Mol Ther 2010;18:1689–1697.
24 Sampaolesi M, Blot S, D'Antona G et al. Mesoangioblast stem cells ameliorate muscle function in dystrophic dogs. Nature 2006; 444:574–579.
25 Darabi R, Gehlbach K, Bachoo RM et al. Functional skeletal muscle regeneration from differentiating embryonic stem cells. Nat Med 2008;14:134–143.
26 Darabi R, Arpke RW, Irion S et al. Human ES- and iPS-derived myogenic progenitors restore DYSTROPHIN and improve contractility upon transplantation in dystrophic mice. Cell Stem Cell 2012;10:610–619.
27 Percival JM, Whitehead NP, Adams ME et al. Sildenafil reduces respiratory muscle weakness and fibrosis in the mdx mouse model of Duchenne muscular dystrophy. J Pathol 2012;228:77–87.
28 Gehrig SM, van der Poel C, Sayer TA et al. Hsp72 preserves muscle function and slows progression of severe muscular dystrophy. Nature 2012;484:394–398.
29 Ono Y, Calhabeu F, Morgan JE et al. BMP signalling permits population expansion by preventing premature myogenic differentiation in muscle satellite cells. Cell Death Differ 2011;18:222–234.
30 Musaro A, Barberi L. Isolation and culture of mouse satellite cells. Methods Mol Biol 2010;633:101–111.
31 Franken NA, Rodermond HM, Stap J et al. Clonogenic assay of cells in vitro. Nat Protoc 2006;1:2315–2319.
32 Fujita R, Kawano F, Ohira T et al. Anti-interleukin-6 receptor antibody (MR16-1) promotes muscle regeneration via modulation of gene expressions in infiltrated macrophages. Biochim Biophys Acta 2014;1840: 3170–3180.
33 Mori M, Nakagami H, Rodriguez-Araujo G et al. Essential role for miR-196a in brown adipogenesis of white fat progenitor cells. PLoS Biol 2012;10:e1001314.
34 Trapnell C, Williams BA, Pertea G et al. Transcript assembly and quantification by RNA-Seq reveals unannotated transcripts and isoform switching during cell differentiation. Nat Biotechnol 2010;28:511–515.
35 Trapnell C, Roberts A, Goff L et al. Differential gene and transcript expression analysis of RNA-seq experiments with TopHat and Cufflinks. Nat Protoc 2012;7:562–578.
36 Huang da W, Sherman BT, Lempicki RA. Systematic and integrative analysis of large gene lists using DAVID bioinformatics resources. Nat Protoc 2009;4:44–57.
37 Huang da W, Sherman BT, Lempicki RA. Bioinformatics enrichment tools: Paths toward the comprehensive functional analysis of large gene lists. Nucleic Acids Res 2009;37:1–13.
38 Nakamura A, Takeda S. Mammalian models of Duchenne muscular dystrophy: Pathological characteristics and therapeutic applications. J Biomed Biotechnol 2011;2011: 184393.
39 Morikawa S, Mabuchi Y, Kubota Y et al. Prospective identification, isolation, and systemic transplantation of multipotent mesenchymal stem cells in murine bone marrow. J Exp Med 2009;206:2483–2496.
40 Morikawa S, Mabuchi Y, Niibe K et al. Development of mesenchymal stem cells partially originate from the neural crest. Biochem Biophys Res Commun 2009;379:1114–1119.
41 Coutu DL, Francois M, Galipeau J. Inhibition of cellular senescence by developmentally regulated FGF receptors in mesenchymal stem cells. Blood 2011;117: 6801–6812.
42 Oh JY, Roddy GW, Choi Het al. Anti-inflammatory protein TSG-6 reduces inflammatory damage to the cornea following chemical and mechanical injury. Proc Natl Acad Sci USA 2010;107:16875–16880.
43 Hagiwara H, Ohsawa Y, Asakura S et al. Bone marrow transplantation improves outcome in a mouse model of congenital muscular dystrophy. FEBS Lett 2006;580:4463–4468.
44 Koning JJ, Kooij G, de Vries HE et al. Mesenchymal stem cells are mobilized from the bone marrow during inflammation. Front Immunol 2013;4:49.
45 Mendez-Ferrer S, Michurina TV, Ferraro F et al. Mesenchymal and haematopoietic stem cells form a unique bone marrow niche. Nature 2010;466:829–834.
46 Omatsu Y, Seike M, Sugiyama T et al. Foxc1 is a critical regulator of haematopoietic stem/progenitor cell niche formation. Nature 2014;508:536–540.
47 Arai F, Hirao A, Ohmura M et al. Tie2/angiopoietin-1 signaling regulates hematopoietic stem cell quiescence in the bone marrow niche. Cell 2004;118:149–161.
48 Kubota Y, Takubo K, Suda T. Bone marrow long label-retaining cells reside in the sinusoidal hypoxic niche. Biochem Biophys Res Commun 2008;366:335–339.
49 Ono Y, Masuda S, Nam HS et al. Slow-dividing satellite cells retain long-term self-renewal ability in adult muscle. J Cell Sci 2012;125:1309–1317.
50 Lee TH, Wisniewski HG, Vilcek J. A novel secretory tumor necrosis factor-inducible protein (TSG-6) is a member of the family of hyaluronate binding proteins, closely related to the adhesion receptor CD44. J Cell Biol 1992;116:545–557.
51 Milner CM, Higman VA, Day AJ. TSG-6: A pluripotent inflammatory mediator? Biochem Soc Trans 2006;34:446–450.
52 Wisniewski HG, Vilcek J. Cytokine-induced gene expression at the crossroads of innate immunity, inflammation and fertility: TSG-6 and PTX3/TSG-14. Cytokine Growth Factor Rev 2004;15:129–146.
53 Heredia JE, Mukundan L, Chen FM et al. Type 2 innate signals stimulate fibro/adipogenic progenitors to facilitate muscle regeneration. Cell 2013;153:376–388.
54 Joe AW, Yi L, Natarajan A et al. Muscle injury activates resident fibro/adipogenic progenitors that facilitate myogenesis. Nat Cell Biol 2010;12:153–163.
55 Uezumi A, Fukada S, Yamamoto N et al. Mesenchymal progenitors distinct from satellite cells contribute to ectopic fat cell formation in skeletal muscle. Nat Cell Biol 2010;12: 143–152.
56 Pisani DF, Clement N, Loubat A et al. Hierarchization of myogenic and adipogenic progenitors within human skeletal muscle. StemCells 2010;28:2182–2194.
57 Wosczyna MN, Biswas AA, Cogswell CA et al. Multipotent progenitors resident in the skeletal muscle interstitium exhibit robust BMP-dependent osteogenic activity and mediate heterotopic ossification. J Bone Miner Res 2012;27:1004–1017.

Send Orders for Reprints to reprints@benthamscience.net

Immun., Endoc. & Metab. Agents in Med. Chem., 2013, *13*, 00-00

Development of LC-MS/MS Quantification of the Novel Antimicrobial Peptide, SR-0379, and its Pharmacokinetics in Rats

Hideki Tomioka[1,2], Hironori Nakagami[3]*, Tomokazu Sano[4], Kazuaki Takafuji[5], Seiji Takashima[5], Yasufumi Kaneda[6] and Ryuichi Morishita[1]*

[1]*Department of Clinical Gene Therapy, Osaka University Graduate School of Medicine, 2-2 Yamada-oka, Suita, Osaka 565-0871, Japan;* [2]*AnGes MG, Inc. 7-7-15 Saito Bio-Incubator, Ibaraki, Osaka 567-0085, Japan;* [3]*Division of Vascular Medicine and Epigenetics, Osaka University United Graduate School of Child Development, 2-1 Yamada-oka, Suita, Osaka 565-0871, Japan;* [4]*Drug Disposition Research Group, Contract Research Department, ADME & Tox. Research Institute, Sekisui Medical Co., Ltd., 2117 Muramatsu, Tokai, Ibaraki, 319-1182, Japan;* [5]*Center for Medical Research and Education, Osaka University Graduate School of Medicine, 2-2 Yamada-oka, Suita, Osaka 565-0871, Japan;* [6]*Division of Gene Therapy Science, Osaka University Graduate School of Medicine, 2-1 Yamada-oka, Suita, Osaka 565-0871, Japan*

Abstract: During the preclinical study of the original functional peptide, SR-0379, a sensitive liquid chromatography-tandem mass spectrometry method was newly developed to study the pharmacokinetics of SR-0379 in rat plasma and subcutaneous tissue samples. Although SR-0379 was unstable in the rat plasma and subcutaneous tissue samples, pretreatment with EDTA and phosphoric acid (4 %) inhibited its degradation. The lower limits of quantification (LLOQ) for SR-0379 were fully validated as 5 ng/ml in plasma and 5 ng/g in tissue with acceptable linearity, intra- and inter-assay precisions, and accuracy. Measurement of SR-0379 concentration in plasma after intravenous injection *via* LC-MS/MS yields plasma concentration-time curves ($AUC_{0-\infty}$) with areas of 667 ng•min/ml and an elimination half-life ($t_{1/2}$) of 4.8 min. The concentration of SR-0379 in the subcutaneous tissue samples was 13.1 μg/g tissue at 30 minutes after a single dermal application (1 mg/ml, 50 μl) to a full-thickness excisional wound. Here, a highly sensitive and specific LC-MS/MS assay with a lower limit of quantification of 5 ng/ml was developed and validated to quantify SR-0379 in rat plasma. This method is useful for pharmacokinetic studies of the peptide drugs in rats.

Keywords: LC-MS/MS, pharmacokinetics, plasma, quantitation, subcutaneous tissue.

INTRODUCTION

While screening of the functional genes for angiogenic molecules *via in silico* analysis, we have developed a novel small, angiogenic peptide with thirty amino acids, named as AG30 [1, 2]. From AG30, we further developed a potent angiogenic peptide with anti-microbial activity, named as SR-0379, which has twenty amino acids (under submission). Because both of anti-microbial and angiogenic actions are required in the wound healing process, SR-0379 might be an effective therapeutic agent to treat the wounds such as decubitus ulcer, diabetic ulcer, and burn ulcers.

Recently, functional peptides and proteins have been considered as potential drugs [3-5]. Bioassays, immunoassays and isotope tracer techniques have been used to evaluate the pharmacokinetics of peptides and proteins [6]. Immunoassays such as ELISA are unable to distinguish such compounds from their metabolites, which is the primary disadvantage of these methods [7]. The total radioactivity detected using an isotope tracer technique is not indicative of the parent compound concentration in biological samples [8]. Mass spectrometry-based technologies can provide many benefits over these methods [9]. The quantitative analysis of peptides and proteins *via* liquid chromatography/mass spectrometry (LC/MS) might be difficult; however, LC/MS methods that utilize a triple quadrupole, ion trap, and quadrupole time-of-flight (Q-Tof) were recently used to quantify peptides [10-12]. Based on these techniques, we have newly developed a sensitive method for determining bioactive peptides in rat plasma and tissues.

*Address correspondence to these authors at the Division of Vascular Medicine and Epigenetics, Osaka University United Graduate School of Child Development; Tel/Fax: +81-6-6879-4142;
E-mail: nakagami@gts.med.osaka-u.ac.jp and Division of Gene Therapy Science, Graduate School of Medicine, Osaka University, 2-2 Yamada-oka, Suita, 565-0871, Japan; Tel: +81-6-6879-3406; Fax: +81-6-6879-3409;
E-mail: morishit@cgt.med.osaka-u.ac.jp

MATERIALS AND METHODS

Reagents

Synthetic SR-0379 was purchased from ILS, Inc. (Tokyo, Japan). An internal standard (purity>99%) containing L-Leucine-$^{13}C_6$ and ^{15}N was purchased from Sigma-Aldrich (Hokkaido, Japan) and used without further purification. All organic solvents were of LC/MS grade and were obtained from Kanto Chemical Co., Inc. (Tokyo, Japan) and Wako Pure Chemical Industries, Ltd. (Osaka, Japan). HPLC grade water was obtained using a water purification system (Auto pure WR600G, Yamato Scientific Co., Ltd, Tokyo, Japan).

1871-5222/13 $58.00+.00

LC-MS/MS Analysis

The HPLC system (LC20AD series, Shimadzu Co., Kyoto, Japan) consisted of a binary pump, autosampler, column oven maintained at 40°C and X Bridge C18 column (2.1 mm × 150 mm, 3.5 µm, Waters, MA, USA). The mobile phase was a mixture of solvent A (0.2% formic acid in MilliQ water) and solvent B (0.2% formic acid in acetonitrile) and used a flow rate of 0.3 ml/min. The following gradient was used for the plasma analyses: hold at 10% B for 0.2 min, increase linearly to 30% B over 2.6 min, then increase to 90% B over 0.2 min, hold for 1.3 min, decrease to 10% B over 0.1 min, hold for 1 min, increase to 90% B for 0.1 min, hold for 1.2 min, decrease to 10% B for 0.1 min, and hold for 2 min. The following gradient was used for the subcutaneous tissue samples: hold at 10% B for 0.2 min, increase linearly to 30% B over 2.8 min, then increase to 90% B over 0.1 min, hold for 0.5 min, decrease to 10% B for 0.1 min, and hold for 1.8 min.

The detection was performed using a QTRAP5500 mass spectrometer (Applied Biosystems Sciex, Framingham, MA, USA) with an ESI source operating in the positive ion mode. Multiple reaction monitoring (MRM) of SR-0379 used the m/z 534.1 → 217.2 transition. The following optimized MS conditions were used: curtain gas (nitrogen), gas 1 (air) and gas 2 (air) in portions of 30, 30 and 30, respectively; ion spray voltage of 4500 V; source temperature of 600°C; declustering potentials of 126 V for SR-0379 and 126 V for IS; collision energies of 29 eV (m/z 534 → 217.2) for SR-0379 and 29 eV (m/z 534.4 → 217.2) for IS.

Optimization of Stability in Plasma

SR-0379 samples (nominal concentrations of 10 and 800 ng/ml) were prepared in blank rat plasma (EDTA). The samples was mixed after adding three times their mass of 4% phosphoric acid. The short-term matrix stability was assessed by analyzing the samples after storing at -80°C, 4°C and room temperature for 24 hours.

Pretreatment of Plasma Samples

A 5-µL aliquot of a SR-0379 working solution in 50% methanol/H_2O at various concentrations (5 – 1000 ng/ml) was mixed with 1500 µl phosphoric acid (4%). Next, 495 µl of rat plasma and 10 µl of the internal standard solution (5000 ng/ml) were added. The solution was vortexed for 10 s and centrifuged at 10,000 × *g* for 5 min. The supernatant was transferred to an Oasis HLB µElution plate that had been previously activated by successive applications of 0.3 ml methanol and 0.3 ml Milli-Q water. This plate was then washed with 0.3 ml of Milli-Q water. The peptide adsorbed onto the surface of the plate was eluted with 150 µl of acetonitrile-water-trifluoroacetic acid (75:25:1). A 10 µl aliquot was transferred to the LC-MS/MS system.

Pretreatment of Subcutaneous Tissue Samples

A 5 µL aliquot of a SR-0379 working solution in 50% methanol/H_2O at various concentrations (5 - 1000 ng/g tissue) was mixed with 750 µl phosphoric acid (4%). Next, 250 µl of a subcutaneous tissue sample (20% homogenate) and 10 µl of an internal standard solution (5000 ng/ml) were added to the above mixture. The solution was vortexed for 10 s and centrifuged at 10,000 × *g* for 5 min. The supernatant was transferred to an Oasis HLB µElution plate that had been activated by successive applications of 0.3 ml of methanol and 0.3 ml of Milli-Q water. The plate was then washed with 0.4 ml of Milli-Q water. The adsorbed peptide was eluted on the surface using 150 µl of acetonitrile-water-trifluoroacetic acid (75:25:1). A 10 µl aliquot was transferred to the LC-MS/MS system.

Method Validation

The method validation evaluated the specificity, linearity, lower limit of quantitation (LLOQ), precision, accuracy, and extraction recovery. The specificity was evaluated based whether an interference peak eluted at the same retention time as for the analytes in a blank sample. The calibration curves were constructed over the SR-0379 concentration range from 5 to 1000 ng/ml for plasma and from 5 to 1000 ng/g for tissue. The intra-assay precision and accuracy were evaluated by replicating five QC samples on the same day. The inter-assay precision and accuracy were evaluated by analyzing QC samples across three separate days. The extraction recovery was determined by comparing to a blank plasma or subcutaneous tissue sample containing analytes added after the pretreatment.

Method Application for a Pharmacokinetic Study in Rats

Male SD rats weighing 250-350 g were used for the following pharmacokinetic studies. SR-0379 (200 µg/kg) was dissolved in saline and administered to the rats *via* a single i.v. bolus injection. Blood samples were collected 2, 5, 10, 15 and 30 min after dosing. SR-0379 (1 mg/ml for 50 µl/rat) was transdermally administered throughout the full depth of the rat skin. Blood samples were collected after 0.5, 1, 2, 4, 8 and 24 hours. Subcutaneous tissue samples were collected after 0.5, 1 and 24 hours. The SR-0379 concentrations in both the plasma and subcutaneous tissues were measured *via* LC-MS/MS. The study was discussed and approved by the Ethics Committee.

RESULTS

LC-MS/MS Analysis

(Fig. **1A**) shows a typical positive ion ESI mass spectrum for SR-0379. The ion peaks at m/z 445.0, 534.1, 667.2 and 889.3 correspond to the 6+, 5+, 4+, 3+ ions, respectively. The 5+ ion showed the highest sensitivity. The product ion spectrum for the 5+ ion is shown in (Fig. **1B**). High collision energies were found to yield intense product ions.

Typical SRM chromatograms were obtained using the blank (0 ng/ml) and the lowest calibration standard (5 ng/ml) in rat plasma (Fig. **2**). No interfering peaks from endogenous substances were observed at the SR-0379 retention times.

Optimization of Short-term Stability in Plasma

The short-term stability of SR-0379 in plasma was assessed by analyzing the samples (10 and 800 ng/ml) after storing at -80°C, 4°C, and room temperature for 24 hours. The normal plasma concentrations (nominal concentrations of 10 and 800 ng/ml) were below the limit of quantification

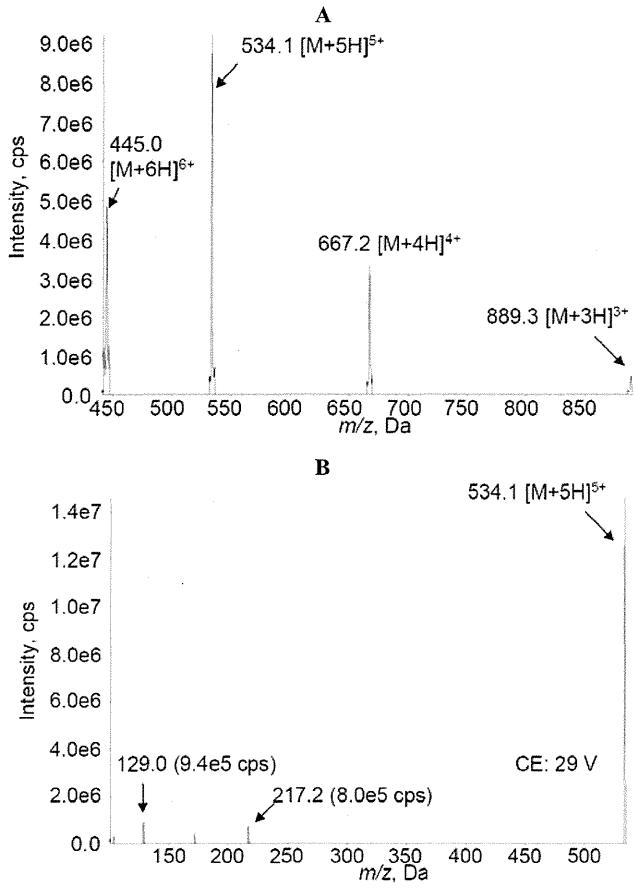

Fig. (1). Positive-ion electrospray mass spectra of SR-0379: (**A**) precursor ion scan and (**B**) product ion mass spectra obtained from [M + 5H]5+ (m/z 534.1).

Table 1. Stability of SR-0379 for 24hr on Each Condition

Nominal Concentration (ng/ml)	Conditions		Observed Value (ng/ml)	RR (%)
			Individual	
10	Normal Plasma	RT	No Peak	-
		4°C	2.89	28.9
		-80°C	9.77	97.7
	4%Phosphoric acid/Plasma (3/1, v/v)	RT	7.32	73.2
		4°C	9.37	93.7
		-80°C	10.2	102.0
800	Normal Plasma	RT	31.6	4.0
		4°C	126	15.8
		-80°C	851	106.4
	4%Phosphoric acid/Plasma (3/1, v/v)	RT	733	91.6
		4°C	848	106.0
		-80°C	891	111.4

and equal to 31.6 ng/ml after storing at room temperature (Table **1**). Thus, SR-0379 was determined to be unstable in

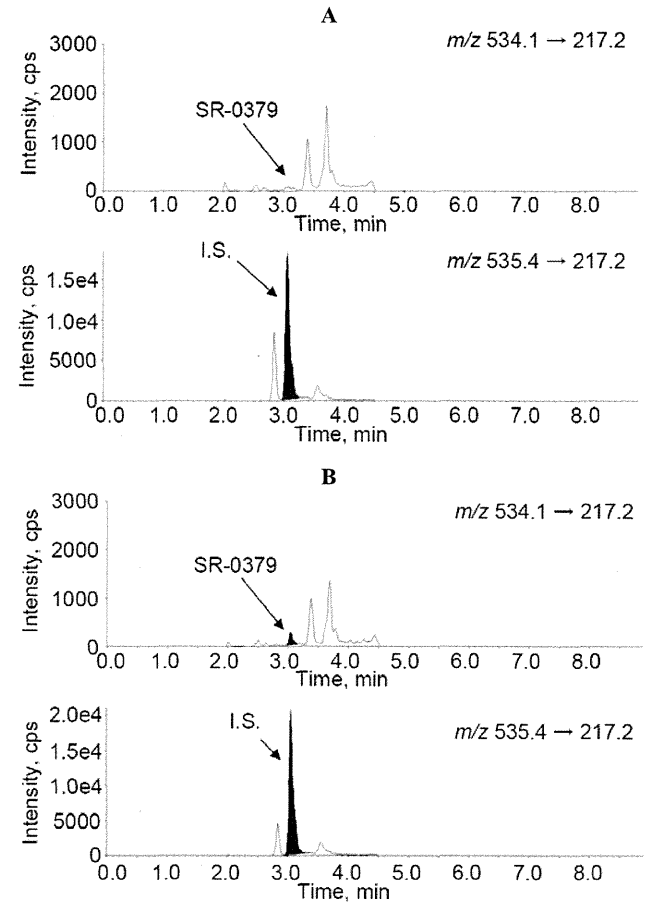

Fig. (2). Selected reaction monitoring ion chromatograms of (**A**) a rat plasma spiked with an internal standard (500 ng/ml) and (**B**) rat plasma spiked with both SR-0379 (5 ng/ml) and the internal standard (500 ng/ml). The SRM transitions were m/z 534.1 → 217.2 for SR-0379 and m/z 535.1 → 217.2 for the internal standard.

rat plasma. Adding 4% phosphoric acid to the plasma sample stabilized the SR-0379. This method development study demonstrated that LC-MS/MS was sufficiently suitable for detecting SR-0379 in 4% phosphoric acid/plasma (3/1, v/v) to proceed with the method validation.

Pretreatment of the Plasma and Subcutaneous Tissue Samples

Solid-phase extraction (SPE) was used as the sample preparation method. During the method development, a variety of SPE cartridges were investigated for both the plasma and subcutaneous tissue sample pre-treatments. Oasis HLB µElution plates provided the highest recovery amongst the SPE cartridges tested.

Method Validation

The specificity was determined by analyzing blank plasma samples from three male rats and three female rats and the pooled plasma of different rats. The assay was linear across the range from 5 to 1000 ng/ml (Table **2**). The lower limit of quantification (LLOQ) in rat plasma was determined to be 5 ng/ml. The within-run CVs were 5.4, 8.9, 6.0 and 5.4% (n=5 for each) for the 5, 10, 50 and 800 ng/ml LLOQ,

Table 2. Linearity of Calibration Curves for the Determination of SR-0379 Concentrations in Rat Plasma

Nominal Concentration (ng/ml)	Back-calculated Value (ng/ml)	RE (%)	Back-calculated Value (ng/ml)	RE (%)	Back-calculated Value (ng/ml)	RE (%)
5	4.94	-1.2	5.06	1.2	4.93	-1.4
10	9.90	-1.0	10.4	4.0	10.2	2.0
20	21.7	8.5	18.6	-7.0	20.2	1.0
50	49.0	-2.0	43.3	-13.4	47.9	-4.2
100	97.6	-2.4	101	1.0	106	6.0
200	190	-5.0	199	-0.5	195	-2.5
800	801	0.1	834	4.3	803	0.4
1000	1030	3.0	1110	11.0	981	-1.9
Correlation coefficient (r)	0.9988		0.9964		0.9993	
Regression formula	$y = 0.00382\,x + 0.000174$		$y = 0.00375\,x - 0.000175$		$y = 0.00391\,x + 0.00140$	
Weighting: $1/x^2$						

Table 3. Intra-day Reproducibility of the QC Samples for the Determination of SR-0379 Concentrations in Rat Plasma

	Nominal Concentration (ng/ml)			
	5	10	50	800
	Observed Value (ng/ml)			
Mean	4.96	10.1	50.1	814
SD	0.27	0.9	3.0	44
CV (%)	5.4	8.9	6.0	5.4
RE (%)	-0.8	1.0	0.2	1.8

respectively (Table **3**). The between-run CVs were 7.4, 8.4, 5.5 and 4.9% (n=15), respectively, for these samples (Table **4**). The within-day and between-day validation parameters meet the FDA Good Laboratory Practice criteria for an analytical method validation.

Pharmacokinetic Study

A profile of the SR-0379 concentration in plasma versus time after an intravenous injection is shown in (Fig. **3A**). The SR-0379 concentration in the plasma rapidly decreased. The pharmacokinetic parameters for SR-0379 are presented in (Table **5**). The area under the concentration to time curve ($AUC_{0-\infty}$) was 667 ng·min/ml, and the obtained elimination half-life ($t_{1/2}$) was 4.8 min.

Table 4. Inter-day Reproducibility of the QC Samples for the Determination of SR-0379 Concentrations in Rat Plasma

Assay date		Nominal Concentration (ng/ml)			
		5	10	50	800
		Observed Value (ng/ml)			
Day 1	1	4.97	10.1	52.5	743
	2	4.55	9.86	45.1	856
	3	5.20	8.86	50.2	802
	4	5.21	10.7	52.4	830
	5	4.89	11.1	50.3	839
Day 2	1	5.29	10.2	50.4	806
	2	5.29	11.0	49.1	849
	3	5.71	10.2	46.7	828
	4	5.86	8.96	52.3	857
	5	5.00	9.08	48.4	849
Day 3	1	5.45	8.63	50.4	757
	2	5.80	10.4	43.7	765
	3	5.64	9.33	46.2	794
	4	5.58	9.76	46.5	782
	5	4.86	8.84	47.8	868
Overall mean (n=15)		5.29	9.80	48.8	815
SD		0.39	0.82	2.7	40
CV (%)		7.4	8.4	5.5	4.9
RE (%)		5.8	-2.0	-2.4	1.9

The SR-0379 concentrations in plasma were below the limit of quantification after a single application of SR-0379 (1 mg/ml, 50 µl) to a full-depth excisional wound. A profile of the subcutaneous tissue concentration versus time for SR-0379 after a single dermal application (1 mg/ml, 50 µl) to a full-depth excisional wound is shown in (Fig. **3B**). The SR-0379 concentration in the subcutaneous tissue samples was 13.1 µg/g tissue at 30 minutes after the application. The concentration in the subcutaneous tissue gradually decreased.

DISCUSSION

In this study, we developed a method for the quantitative analysis of a functional peptide, SR-0379, in rat plasma and tissue using LC/MS with an ion trap [10- 12].

These peptides are unstable in biological fluids, such as plasma and urine [13, 14]. EDTA, a metalloproteinase inhibitor, can be added to the samples to prevent their degradation when determining the concentration [15]. In this study, the stability of SR-0379 spiked into plasma was investigated.

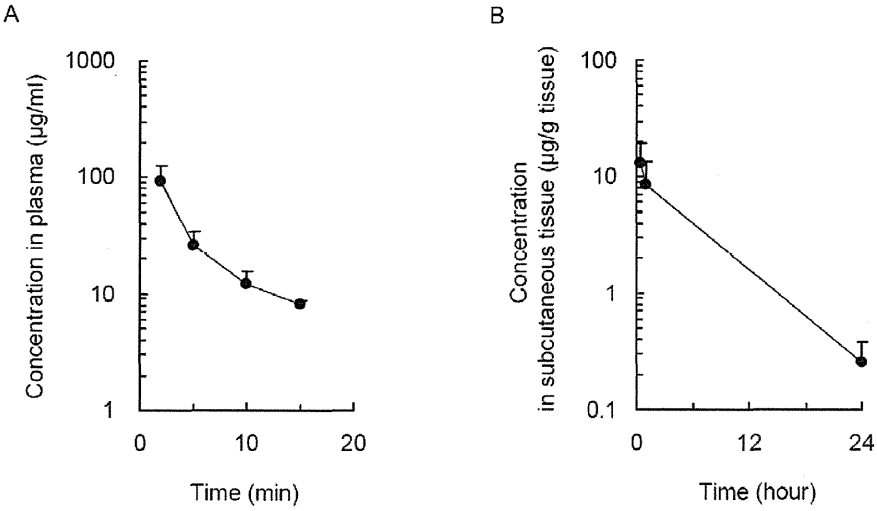

Fig. (3). (**A**) Curve of the plasma concentration versus time after the intravenous administration of SR-0379 (200 μg/kg) to the rats. N=4 per group. (**B**) Curve of the subcutaneous tissue concentration versus time after the dermal application of SR-0379 (1 mg/ml, 50 μl) to a full-depth wound in the rat skin. N=4 per group.

Table 5. PK Parameters of SR-0379 in Rat Plasma after Single Intravenous Administration of SR-0379 to Intact Skin Rats (Group 1, Dose: 200 μg/kg)

Parameters	
$t_{1/2}$ (min)	4.8
$AUC_{0\text{-}t}$ (ng·min/ml)	626
$AUC_{0\text{-}\infty}$ (ng·min/ml)	667
C_0 (ng/ml)	217
CL_{total} (ml/min/kg)	300
Vd (ml/kg)	922
Vd = Dose (ng/kg) / C_0 (ng/ml)	

The results indicated that SR-0379 was unstable in plasma even with EDTA. 4% phosphoric acid was added to improve the stability of SR-0379. Thus, a simple method for determining peptides in biological matrices was established.

The objective of this study was to characterize the pharmacokinetics of SR-0379 using this LC-MS/MS technology. The SR-0379 concentration decreased rapidly following a single intravenous injection of 2 μg/kg into male rats, and an elimination half-life ($t_{1/2}$) of 4.8 min was obtained. SR-0379 has numerous biological activities that are important to wound healing and this peptide is being developed for topical use to treat diabetic, burn and other incurable ulcers. The terminal half-lives ($t_{1/2\beta}$) ranged from 5.0 to 7 min after administering human basic fibroblast growth factor (FGF2) intravenously to mice in doses of 2.5, 5, 10 μg/kg [16]. The stability of SR-0379 is comparable to that of growth factors such as FGF2.

The SR-0379 concentration in rat plasma was below the limit of quantification after a single dermal application (1 mg/ml, 50 μl) to a full-depth excisional wound. Topical treatments have the advantages of avoiding adverse systemic effects while increasing concentration at the target site. In contrast, the SR-0379 concentration in the subcutaneous tissue was 13.1 μg/g of tissue 30 min after its application (1 mg/ml, 50 μl) to a full-depth excisional wound. The concentration in the subcutaneous tissue gradually decreased. It was suggested that the SR-0379 degraded locally.

A highly sensitive and specific LC-MS/MS assay with a lower limit of quantification (LLOQ) of 5 ng/ml was developed and validated to quantify SR-0379 in rat plasma. The lower limit of quantification of hepcidin-25 and ramoplanin was 5 ng/ml and 10 ng/ml, respectively [17, 18]. Most bioanalytical assays for peptides show an LLOQ between 0.5 and 10 ng/ml, with some lower LLOQs mainly for smaller peptides. Lower LLOQ of SR-0379 has achieved by using QTRAP5500 mass spectrometer. This method was fully validated and possessed acceptable linearity, accuracy, and both intra- and inter-assay precisions. Furthermore, this method is useful for performing pharmacokinetic studies in rats.

CONFLICT OF INTEREST

Ryuichi Morishita is a founder and stockholder of AnGes MG. The Department of Clinical Gene Therapy is financially supported by AnGes MG, Novartis, Shionogi, Boehringer and Rohto. The Division of Vascular Medicine and Epigenetics is financially supported by Bayel.

ACKNOWLEDGEMENTS

This study was partially supported by a Health Labour Sciences Research Grant in Japan.

REFERENCES

[1] Nishikawa, T.; Nakagami, H.; Maeda, A.; Morishita, R.; Miyazaki, N.; Ogawa, T.; Tabata, Y.; Kikuchi, Y.; Hayashi, H.; Tatsu, Y.; Yumoto, N.; Tamai, K.; Tomono, K.; Kaneda, Y. Development of a novel antimicrobial peptide, AG-30, with angiogenic properties. *J. Cell. Mol. Med.*, **2009**, *13*, 535-546.

[2] Nakagami, H.; Nishikawa, T.; Tamura, N.; Maeda, A.; Hibino, H.; Mochizuki, M.; Shimosato, T.; Moriya, T.; Morishita, R.; Tamai,

K.; Tomono, K.; Kaneda, Y. Modification of a novel angiogenic peptide, AG30, for the development of novel therapeutic agents. *J. Cell. Mol. Med.*, **2012**, *16*(7), 1629-1639.

[3] Eckert, R. Road to clinical efficacy: challenges and novel strategies for antimicrobial peptide development. *Future Microbiol.*, **2011**, *6*(6), 635-651.

[4] Fjell, C.D.; Hiss, J.A.; Hancock, R.E.; Schneider, G. Designing antimicrobial peptides: form follows function. *Nat. Rev. Drug Discov.*, **2012**, *11*(1), 37-51.

[5] Li, Y.; Xiang, Q.; Zhang, Q.; Huang, Y.; Su, Z. Overview on the recent study of antimicrobial peptides: origins, functions, relative mechanisms and application. *Peptides*, **2012**, *37*(2), 207-215.

[6] Jiang, S.Y.; Jiao, J.; Zhang, T.T.; Xu, Y.P. Pharmacokinetics study of recombinant hirudin in the plasma of rats using chromogenic substrate, ELISA, and radioisotope assays. *PLoS One*, **2013**, *8*(6), e64336.

[7] Wang, Y.; Qu, Y.; Bellows, C.L.; Ahn, J.S.; Burkey, J.L.; Taylor, S.W. Simultaneous quantification of davalintide, a novel amylin-mimetic peptide, and its active metabolite in beagle and rat plasma by online SPE and LC-MS/MS. *Bioanalysis*, **2012**, *4*(17), 2141-2152.

[8] Sands, H.; Li, J.; Duggaraju, R.; Kolan, H.R.; Donegan, M.; Elove, G.A.; Thakur, M.L. Biodistribution and pharmacokinetics of 131I-labeled LEX 032, a recombinant hybrid of antichymotrypsin. *Drug Metab. Dispos.*, **1997**, *25*(5), 631-636.

[9] Liu, Z.; Ren, C.; Jones, W.; Chen, P.; Seminara, S.B.; Chan, Y.M.; Smith, N.F.; Covey, J.M.; Wang, J.; Chan, K.K. LC-MS/MS quantification of a neuropeptide fragment kisspeptin-10 (NSC 741805) and characterization of its decomposition product and pharmacokinetics in rats. *J. Chromatogr. B. Analyt. Technol. Biomed. Life Sci.*, **2013**, *926*, 1-8.

[10] Vatansever, B.; Lahrichi, S.L.; Thiocone, A.; Salluce, N.; Mathieu, M.; Grouzmann, E.; Rochat, B. Comparison between a linear ion trap and a triple quadruple MS in the sensitive detection of large peptides at femtomole amounts on column. *J. Sep. Sci.*, **2010**, *33*(16), 2478-2488.

[11] Miyachi, A.; Murase, T.; Yamada, Y.; Osonoi, T.; Harada, K. Quantitative analytical method for determining the levels of gastric inhibitory polypeptides GIP1-42 and GIP3-42 in human plasma using LC-MS/MS/MS. *J. Proteome Res.*, **2013**, *12*(6), 2690-2699.

[12] Michalski, A.; Damoc, E.; Lange, O.; Denisov, E.; Nolting, D.; Muller, M.; Viner, R.; Schwartz, J.; Remes, P.; Belford, M.; Dunyach, J.J.; Cox, J.; Horning, S.; Mann, M.; Makarov, A. Ultra high resolution linear ion trap Orbitrap mass spectrometer (Orbitrap Elite) facilitates top down LC MS/MS and versatile peptide fragmentation modes. *Mol. Cell. Proteomics*, **2012**, *11*(3), O111.013698.

[13] De Spiegeleer, B.; Van Dorpe, S.; Vergote, V.; Wynendaele, E.; Pauwels, E.; Van De Wiele, C.; Garcia-Solis, P.; Solis-Sainz, J.C. *In vitro* metabolic stability of iodinated obestatin peptides. *Peptides*, **2012**, *33*(2), 272-278.

[14] Ocak, M.; Helbok, A.; Rangger, C.; Peitl, P.K.; Nock, B.A.; Morelli, G.; Eek, A.; Sosabowski, J.K.; Breeman, W.A.; Reubi, J.C.; Decristoforo, C. Comparison of biological stability and metabolism of CCK2 receptor targeting peptides, a collaborative project under COST BM0607. *Eur. J. Nucl. Med. Mol. Imaging*, **2011**, *38*(8), 1426-1435.

[15] Alebic-Kolbah, T.; Demers, R.; Cojocaru, L. Dalbavancin: Quantification in human plasma and urine by a new improved high performance liquid chromatography-tandem mass spectrometry method. *J. Chromatogr. B. Analyt. Technol. Biomed. Life Sci.*, **2011**, *879*(25), 2632-2641.

[16] Zhang, Q.; Wang, G.J.; Sun, J.G. Pharmacokinetics of recombinant human basic fibroblast growth factor in rabbits and mice serum and rabbits aqueous humor. *Acta Pharmacol. Sin.*, **2004**, *25*(8), 991-995.

[17] Murao, N.; Ishigai, M.; Yasuno, H.; Shimonaka, Y.; Aso, Y. Simple and sensitive quantification of bioactive peptides in biological matrices using liquid chromatography/selected reaction monitoring mass spectrometry coupled with trichloroacetic acid clean-up. *Rapid Commun. Mass Spectrom.*, **2007**, *21*(24), 4033-4038.

[18] Ewles, M.F.; Turpin, P.E.; Goodwin, L.; Bakes, D.M. Validation of a bioanalytical method for the quantification of a therapeutic peptide, ramoplanin, in human dried blood spots using LC-MS/MS. *Biomed. Chromatogr.*, **2011**, *25*(9), 995-1002.

Received: November 14, 2013 Revised: November 15, 2013 Accepted: November 18, 2013